Available online at www.sciencedirect.com
SCIENCE DIRECT®
Combustion and Flame 145 (2006) 663–674
Combustion and Flame
www.elsevier.com/locate/combustflame

Substantiating a fractal-based algebraic reaction closure of premixed turbulent combustion for high pressure and the Lewis number effects

Naresh K. Aluri [a], S.P. Reddy Muppala [a,1], Friedrich Dinkelacker [a,b,*]

[a] *Lehrstuhl für Technische Thermodynamik, Universität Erlangen-Nürnberg, Am Weichselgarten 8, 91058 Erlangen, Germany*
[b] *Institut für Fluid- und Thermodynamik, Universität Siegen, Paul-Bonatz-Str. 9, 57068 Siegen, Germany*

Received 29 April 2005; received in revised form 30 August 2005; accepted 8 February 2006

Available online 24 March 2006

Abstract

A comprehensive set of nearly 100 atmospheric and high-pressure flame data of Kobayashi et al. are a good source for numerical analysis to address two main aspects in premixed turbulent combustion—high-pressure influence and effects of fuel type on the reaction rate. The present work deals with the lucid and realizable fractal-based reaction rate closure from Lindstedt and Váos (LV model) for premixed flames in the thin-flame limit. In this study, the reaction source term is customized on the eddy viscosity closure of turbulent transport, for practical reasons. Computed results from the LV model show the right qualitative trends with the experimental findings, as a function of turbulence. However, quantitative predictions of the original model are partly too low, and preclude the effects of pressure and fuel type on the reaction rate. With an extensive parametric study, based on numerical findings as well as on theoretical argumentation, the LV model is substantiated for these two effects. Results from the proposed tuned LV model are found to be in very good agreement with most of the measured data.
© 2006 The Combustion Institute. Published by Elsevier Inc. All rights reserved.

Keywords: Turbulent premixed combustion; Numerical reaction rate modeling; High-pressure flames; Turbulence scales; Lewis number

1. Introduction

In modeling premixed turbulent combustion, two major challenges are to be met: turbulence modeling and reaction rate modeling [1]. In complex flow situations, such as swirling flows and recirculating flows, interaction of turbulence and reaction is a nontrivial question. The present study encounters a relatively simple flow situation of Bunsen flames with exit velocities mostly in the range of a few m/s, without strong flow gradients in the flame region. Therefore, in this paper, we consolidate investigation of the fundamental turbulent combustion processes, focusing mainly on reaction-rate modeling. On the other hand, operating pressures beyond atmospheric levels in premixed turbulent combustion are rewarding, with application to large-scale industrial devices such as gas-turbine combustors and internal combustion engines.

* Corresponding author. Fax: +49 271 740 2360.
E-mail address: dinkelacker@ift.mb.uni-siegen.de (F. Dinkelacker).
[1] Now with Département de Mécanique, TERM, Université Catholique de Louvain, Place du Levant, 2, 1348 Louvain-la-Neuve, Belgium.

0010-2180/$ – see front matter © 2006 The Combustion Institute. Published by Elsevier Inc. All rights reserved.
doi:10.1016/j.combustflame.2006.02.004

Nomenclature

A	fractal area
A_T	turbulent flame surface area
$\bar{A}$	averaged flame surface area
C_R	a preconstant (reaction rate parameter)
$\tilde{c}$	Favre-averaged reaction progress variable
$\bar{c}$	Reynolds-averaged reaction progress variable
$C_{P,Le}$	a prefactor for pressure and Lewis number effects
D	fractal dimension
Da	Damköhler number
E_A	activation energy
Ka	Karlovitz number
$\tilde{k}$	turbulent kinetic energy
l^3	volume of flame element
l_λ	Taylor length scale, $l_x\,\mathrm{Re}_t^{-0.5}$
l_k	Kolmogorov length scale, $(\nu^3/\varepsilon)^{1/4}$
l_x	integral length scale
Le	Lewis number of the fuel–air mixture
p	operating pressure
P_R	probability of occurrence of reaction
Re_t	turbulent Reynolds number, $u' l_x/\nu$
s_L	unstretched laminar flame speed
s_T	turbulent flame speed
U	mean inlet flow velocity
u'	r.m.s. turbulent velocity
$\tilde{u}_i$	Favre-averaged component of the gas flow velocity **u**
u_i''	fluctuating component of the gas flow velocity **u**
$\overline{u''c''}$	turbulent flux
V_K	Kolmogorov velocity, $(\nu_0\varepsilon)^{1/4}$
$\bar{w}_c$	mean chemical reaction rate

Greek letters

γ	unburned to burned density ratio
δ_L	laminar flame thickness
δ_T	turbulent flame brush thickness
ε_i	inner cut-off scale
ε_o	outer cut-off scale
$\tilde{\varepsilon}$	dissipation rate
μ	molecular dynamic viscosity
μ_t	turbulent viscosity
ν	molecular kinematic viscosity
ν_u	(unburned) molecular kinematic viscosity
ν_t	turbulence exchange coefficient
ν^*	normalized pressure-variant kinematic viscosity, $\nu(p)/\nu(p_0)$
ρ	density of gas
ρ_u	(unburned) density of premixed mixture
ρ_b	(burned) density of reaction products
Σ	flame surface density
σ_c	turbulent Schmidt number
ϕ	equivalence ratio

Notwithstanding its very significant role, the influence of pressure on turbulent flame speed/reaction rate is barely attended due to the associated difficulties in performing defined experiments. Evolution of suitable measurement data for numerical validation has therefore been slow albeit promising [2–6]. The present focus is on two important subjects, not much regarded in the past: the influence of pressure and fuel effects on reaction closure. In general, a numerical model should be able to account for both these effects, to claim generality of the model. However, quite often, numerical models are validated over a small range of conditions, mainly restricted to atmospheric methane flames.

In the last years, our attempt has been to investigate some of the well-known existing models for turbulent premixed combustion for the influence of pressure and fuel type. This paper shows results from one of a series of similar studies, which are based on this broad set of experimental data of Kobayashi et al. Different models for turbulent premixed flames have been tested recently [7–9] based on turbulent flame-speed closure [10], BML-type models [11,12], and flame surface density models [13–15]. These models respond only weakly to the aforesaid effects. In a recent study, a three-parameter algebraic reaction rate closure for the flame-wrinkling ratio $A_T/\bar{A}$ was developed with the reaction progress variable gradient approach [16], by including explicit high-pressure effects and an empirical 1/Le dependency to describe the influence of nonunity Lewis number. The importance of the Lewis number to turbulent reaction rates was discussed elaborately in a recent review by Lipatnikov and Chomiak [17], including similar Le-dependency[2] findings from detailed numerical simu-

[2] Very recently, Chen and Bilger [18] reported observations on the differences of the curvature distribution, on the conditional mean scalar dissipation rate, and on the extinction behavior between lean propane–air and methane–air flames, which they attribute to difference in the Lewis numbers between the two. Experimental studies by Renou et al. [19] and by Brutscher et al. [20] show alternative relations between the Markstein length and the flame behavior.

lation [21], on the importance of molecular transport effects associated to highly turbulent flames.

In [9], two algebraic reaction rate models from Lindstedt and Váos (LV) [12] and Bray–Moss–Libby (BML) [11] were numerically evaluated with the experimental data of Kobayashi, for nonunity Le flames at 1 bar. The predictive capabilities of the two models are well preserved for the methane/air flames by tuning the model preconstant in the LV closure and by slightly altering the exponent value of the wrinkling length scale L_y in the BML-model. To include the influence of different fuels, the mean reaction rate closures were substantiated by inclusion of an explicit 1/Le factor, for improved numerical findings. Prediction of flame shape and brush thickness, however, suggested a preference for the LV closure [9], supported by the qualitative shapes of the experimental flames of Kobayashi. We therefore restricted to the further investigation of the simple-structured Lindstedt and Váos reaction closure, with a special interest to the influence of pressure and fuel type.

The present numerical analysis is facilitated by the extensive set of Kobayashi flame data [2,22,23] at high pressure and varied degree of turbulence on three gaseous hydrocarbon fuels. These data were obtained for operations up to 30 bar, involving more than 100 flames [24]. Nozzle exit velocities (of the premix mixture) ranged between 0.86 and 8.86 m/s, with geometrical Reynolds numbers (based on nozzle exit diameter) up to 115,000; turbulence r.m.s. velocity and transverse integral length scale up to 2.06 m/s and 1.90 mm, respectively. The data set involved three gaseous hydrocarbon fuels, with lean methane/air mixtures of $\phi = 0.9$ for 1, 5, 10, 20, and 30 bar, ethylene/air with $\phi = 0.5$, 0.7, and 0.9 for 1, 5, and 10 bar, and propane/air $\phi = 0.9$ for 1 and 5 bar. The experimental averaged shape of a Bunsen flame was determined using the schlieren technique from the ensemble average of 50 instantaneous images for every flame. Typical average cone angle was determined for each flame from the location with a 50% probability of finding burned gas. In Fig. 1, the experimental data are shown in a premixed turbulent regime diagram. While some of the flames (especially at weak pressure) fall into the classical flamelet regime C, the high-pressure flames are expected to take corrugated or thickened flame fronts, following older theories. However, both direct numerical simulations [25,26] and evaluation of some of the detailed experiments [27–29] and theoretical evaluations [29–31] show an increased spread of the thin flame regime, especially if the turbulent Reynolds number is not too high. Within this thin flame regime, reaction is assumed to occur in asymptotically thin layers with a well-defined inner structure corresponding to that of stretched laminar flame. The instantaneous composition field is postulated to consist of regions of either unburned or completely burned gas, separated by thin wrinkled or corrugated interfaces. And, as s_L is a strong decreasing function of pressure, higher ratios of turbulence–chemistry interactive term u'/s_L reaching partly up to at elevated pressures.

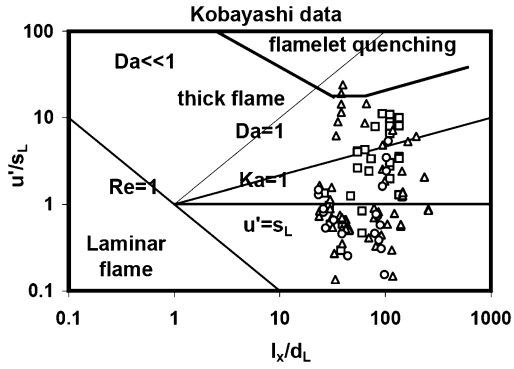

Fig. 1. Full set of experimental data of Kobayashi et al. [2,22,23], along with the boundary of flamelet quenching, and thick flame in the modified phase diagram of turbulent premixed combustion. Methane (□), ethylene (△), and propane (○).

Increase of pressure is known to influence both turbulence as well as laminar premixed flame characteristics. Experimentally observed flames are more wrinkled at increased pressure [2–4], where especially smaller turbulence scales (Taylor scale, Kolmogorov scale) decrease, while the turbulent integral scale remains nearly unaffected by pressure. This can be understood from the classical turbulence theory, based on decrease of kinematic viscosity $\nu = \mu/\rho$ with pressure. Thus, increased pressure induces higher turbulent Reynolds number, $\mathrm{Re_t} = u' l_x/\nu$ (if the mean velocity is held constant, typically the turbulence intensity u' is also only weakly affected by pressure). The small scales of turbulence depend inversely on the turbulent Reynolds number (Taylor scale $l_\lambda \propto l_x/\mathrm{Re_t^{0.5}}$; Kolmogorov scale $l_k \propto l_x/\mathrm{Re_t^{0.75}}$; l_x is the integral length scale). Correspondingly, measured energy spectra on turbulence show a shift to higher frequency regions [2]. On the other hand, the structure of laminar flames also depends on pressure. It is known from detailed laminar flame calculations that the laminar flame speed decreases with increase of pressure. It is approximated for methane as $s_L \propto p^{-0.5}$, and for ethylene and propane as $s_L \propto p^{-0.25}$. The laminar flame thickness also decreases with increasing pressure, depending on the details of the local transport and reaction processes, where asymptotic theories predict a dependency such as $\delta_L \propto \alpha/s_L \propto \nu/s_L$ [32]. The kinematic viscosity can thus be featured as a fundamental parameter relating the influence of pressure on flame characteristics. It is of particular inter-

est to note that the mean reaction rate of premixed turbulent flames increases with pressure, despite decrease in s_L. This is the result of pressure effects on turbulence-induced flame wrinkling and laminar flame and is discussed in more detail in the frame of this study.

With a short introduction to the LV reaction model, the work is organized as follows. Numerical results of lean methane/air flames (Le = 1) followed by lean ethylene and propane/air flames (Le > 1) at 1 bar are convened. In a successive step, the influence of high pressure is investigated for three-fuel flame data. Based on comparisons between calculated and experimental flame angles, the LV model is "tuned" to include the influence of pressure and fuel. For the latter, a simple 1/Le-relation found in a previous study is exchanged with the more elaborate dependent term. Some theoretical discussion for the devised "tuned" Lindstedt–Váos (tLV) model with its pressure dependencies is given based on the KPP-analysis of the integrated reaction rate in the frame of turbulent flame speed. In a supportive study, the cross-influence of the turbulent viscosity model is investigated for some representative flames for two Schmidt number values and for the behavior of the reaction closure under spatially uniform turbulence fields. Finally, advantages as well as limits of the substantiated reaction closure are discussed.

2. Numerical reaction model

2.1. Reaction progress variable

As turbulent premixed flames are often characterized by thin reaction zones [33], the mass fractions of the species and temperatures may be expressed as a function of a single reduced progress variable, c ($c = 0$ within fresh reactants and $c = 1$ within burned products). The transport equation for the Favre-averaged (mass-weighted) progress variable $\tilde{c}$ takes the form

$$\frac{\partial}{\partial x_j}(\bar{\rho}\tilde{u}_j\tilde{c}) + \frac{\partial}{\partial x_j}\left(\widetilde{\bar{\rho}u_j''c''}\right) = \overline{\nabla(\zeta)} + \bar{w}_c, \tag{1}$$

where $\bar{w}_c$ is the mean chemical reaction rate. The contribution of molecular diffusion ζ is usually neglected for high-Reynolds-number flows. The second term describes the turbulent flux, which is modeled using the classical *gradient-transport* assumption, $\bar{\rho}u''c'' = -(\bar{\rho}\nu_t/\sigma_c)\nabla\tilde{c}$, where σ_c is the turbulent Schmidt number. Thus, for steady state conditions, Eq. (1) reads as

$$\frac{\partial}{\partial x_j}(\bar{\rho}\tilde{u}_j\tilde{c}) = \frac{\partial}{\partial x_j}\left(\bar{\rho}\frac{\nu_t}{\sigma_c}\frac{\partial\tilde{c}}{\partial x_j}\right) + \bar{w}_c. \tag{2}$$

2.2. The reaction rate model

Assuming that reaction occurs in thin flame sheets separating unburned and burned gases, $\bar{w}_c$ may be expressed as the product of the flame surface area per unit volume Σ and the laminar flame speed s_L:

$$\bar{w}_c = \rho_u \cdot s_L \cdot \Sigma. \tag{3}$$

One major advantage of this approach is in decoupling chemistry from the flame–turbulence interaction described by Σ. Of many possibilities in modeling this complex term Σ (e.g., [10,14,30,34–38]), the fractal concept from which the LV reaction model was derived is discussed in the following. This LV model belongs to the genre of algebraic models. It was developed on the assumption that the flame surface geometry is fractal [34], following a self-similarity power law between an inner and an outer cut-off scale. The fractal theory was applied to evaluate the increase in flamelet surface area due to turbulent eddies. The mean flame surface density $\langle\Sigma\rangle$ is

$$\langle\Sigma\rangle \equiv A/l^3\frac{1}{l}\left(\frac{\varepsilon}{l}\right)^{2-D}, \tag{4}$$

with $2 < D < 3$. For its compatibility with the diffusive/dissipative characteristics of passive or reactive scalars, a finite limit for the surface area is established, with an inner cut-off ε_i introduced such that $l_x \geqslant \varepsilon \geqslant \varepsilon_i$. Gouldin and Dandekar [39] have argued for identifying the inner cut-off scale as the Kolmogorov length scale (i.e., $\varepsilon_i = l_k$). Similarly, to accommodate for the geometrical constraints, the largest self-similar scale of wrinkling is related to the l_x, with outer cut-off $\varepsilon_o \cong l_x$, so that $l \geqslant \varepsilon_o \geqslant \varepsilon \geqslant \varepsilon_i$. To ensure isotropicity and for l to be at least equal to the expected largest scale of wrinkles, $l = \varepsilon_o = l_x$. Thus,

$$\langle\Sigma\rangle \propto \frac{1}{l_x}\left(\frac{l_k}{l_x}\right)^{2-D}P_R, \tag{5}$$

where P_R is the probability of reaction occurring within the volume under consideration. For the probability of reaction, following [40], Lindstedt and Váos used the empirical relation satisfying the extremum flame boundary conditions $c = 0$ and $c = 1$ across the flame front for the flamelet regime of combustion:

$$P_R = \tilde{c}(1-\tilde{c}). \tag{6}$$

Lindstedt and Sakthitharan [41] proposed D equal to 7/3. Substituting this value into Eq. (6), with the introduction of Kolmogorov velocity V_K and assuming $l_x \propto \tilde{k}^{3/2}/\tilde{\varepsilon}$, the Lindstedt–Váos (LV) reaction model is [12]

$$\bar{w}_c = C_R\rho_u\frac{s_L}{V_K}\frac{\tilde{\varepsilon}}{\tilde{k}}\tilde{c}(1-\tilde{c}), \tag{7}$$

where C_R is the model constant.

The critical assumption implicit in the derivation of the above expression is that vortices of all sizes between the integral and the inner cut-off Kolmogorov length scales [34] contribute to the wrinkling of the flame surface. Gülder et al. [42] found from other experiments the fractal dimension D to be 2.2, rather than 2.33, used in the LV model (see also [43,44]). Other expressions found in literature relate the inner cut-off to the Gibson scale [33] or the laminar flame thickness δ_L [45]. The quantity s_L/V_K is stated to represent the relation between reacting (laminar flame propagating with s_L) and passive scalars (turbulent mixing). Lindstedt and Váos set the reaction rate parameter $C_R = 2.6$ to reach quantitative agreement with counterflow experiments [12]. The exact value seemed to depend on the flame geometry [46]. Additionally, it should be noted that Lindstedt and Váos modeled the turbulent flux term with a second moment closure, while in the following study a simpler eddy viscosity approach is used. Váos investigated the cross influence between the turbulent flux model and the reaction model [46]. For an increased C_R value, the simple eddy viscosity approach gave reasonable results ($C_R = 3.25$ for the eddy viscosity approach compared to $C_R = 1.5$ for the second moment closure for the discussed experimental data [47]). We conclude that the eddy viscosity closure for turbulent flux in the combustion progress variable transport equation is an acceptably practiced approach, at least as long as the prediction of flame brush thickness is not the central focus.

Together with the transport equation for $\tilde{c}$, this reaction model is implemented via subroutines into the commercial finite-volume-based computational fluid dynamics code [48], solving for the Favre-averaged Navier–Stokes equations. Pressure–density coupling is based on the SIMPLE algorithm, and turbulence is modeled with the standard formulation of the k–ε model. The following relations link the theoretical turbulence properties and the calculated turbulence quantities k and ε,

$$u' = \sqrt{\tfrac{2}{3}\tilde{k}}, \qquad l_x = c_\mu^{3/4}\frac{\tilde{k}^{3/2}}{\tilde{\varepsilon}}, \qquad \nu_t = c_\mu\frac{\tilde{k}^2}{\tilde{\varepsilon}}, \quad (8)$$

with $c_\mu = 0.09$ and ν_t the turbulent kinematic viscosity.

With the thin flame assumption, the following mean density relation is shown to be valid [49]:

$$\frac{1}{\bar{\rho}(\tilde{c})} = \frac{1-\tilde{c}}{\rho_u} + \frac{\tilde{c}}{\rho_b}. \quad (9)$$

Both ρ_u and ρ_b are fed to the solver as input, assuming adiabatic flame conditions. In a post processing step, calculated $\tilde{c}$ is transformed to $\bar{c}$ using

$$\bar{c} = \frac{(1+\tau)\tilde{c}}{1+\tau\tilde{c}}, \quad (10)$$

with the heat release parameter $\tau = (\rho_u/\rho_b - 1)$ [11]. This conversion is necessitated for direct comparison with the experimental data available in Reynolds-averaged form. Note that the difference between Reynolds-averaged and Favre-averaged flames is remarkable for a Bunsen flame [9]. In an earlier study [50], the grid dependency was investigated for one typical flame. Only a weak influence of the grid resolution (by varying the number of cells per cm between 5 and 50 corresponding to a number of total grid volumes slightly above 60,000) on the calculated flame cone angle was found. Therefore, in the following study also a grid resolution of 25 cells/cm is used on a two-dimensional axisymmetric computational domain, corresponding to 75×200 grid points.

3. Investigation of the fractal-based reaction model from Lindstedt and Váos

Calculations are performed for a wide range of data—three fuels (CH_4, C_2H_4, and C_3H_8), varied turbulence levels (u'/s_L as high as 25), and pressures up to as high as 30 bar. Simulated results obtained from the LV model (Eq. (7)) are compared with the experimental counterparts, and the merits and limitations of the model are elucidated. Comparisons are made for the flame cone angle, estimated through the optimal tangent drawn over the $\bar{c} = 0.5$ contour of the Reynolds-averaged reaction progress variable. Using the flame angle method, a turbulent flame speed may be used as a representative of the flame cone angle, $s_T = U\sin(\theta/2)$. In the following, the flame angles are mostly presented in the nondimensional s_T/s_L form. This term also may be interpreted as an approximation of the ratio between turbulent and laminar reaction rates.

3.1. Influence of fuel

In Fig. 2, the calculated flame cone angles obtained from the LV model of Eq. (7) with $C_R = 2.6$ are compared with the corresponding measured data at 1 bar. This clearly shows that the model is able to predict the flame speed variation qualitatively with turbulence. Comparing the methane–air flames with the increase of u'/s_L from 0.3 to 1.35, deviations enlarge, an indication of the nonapplicability of the original constant $C_R = 2.6$. Additionally, this figure shows that all calculated flames of methane–air, ethylene–air (equivalence ratio $\phi = 0.7$ and 0.9; Le = 1.2), and propane–air ($\phi = 0.9$; Le = 1.62) essentially fall onto a straight line, while the experimental data differ significantly. While the reaction rate (being proportional to s_T/s_L) is underpredicted

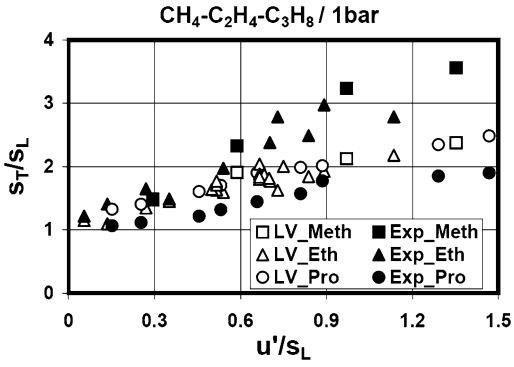

Fig. 2. Comparison of calculated flame angle in s_T/s_L from the LV model with the experimentally measured data of Kobayashi for methane ($\phi = 0.9$), ethylene ($\phi = 0.7$ and 0.9), and propane ($\phi = 0.9$) flames at 1 bar.

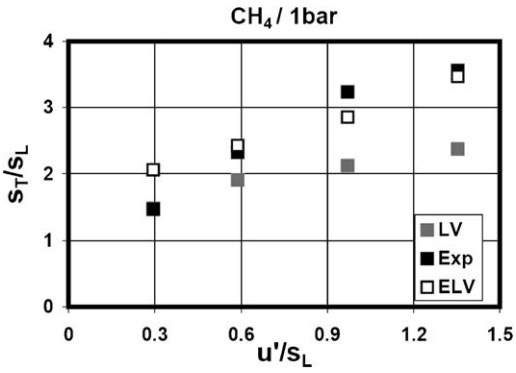

Fig. 3. Methane–air flames ($\phi = 0.9$) at 1 bar from the tLV model. Also included are results from the LV model for comparison.

for methane flames, and to a lesser extent for ethylene flames, it is slightly overpredicted in the case of propane flames. Obviously the numerical model is insufficient to elucidate the fuel effects in this form. Before overseeing the expansion of the LV model, (Section 4, with results in Figs. 3 and 4), the influence of pressure on the LV model is discussed.

3.2. High-pressure influence

The influence of pressure on turbulent flame speed is also studied, being of practical interest such as to gas-turbine combustors. It was evident from experiments that as pressure rises (from 5 to 30 bar), s_T/s_L increase with u'/s_L. Calculations performed for pressures 5, 10, 20, and 30 bar consist of 5, 4, 10, and 7 methane–air flames, respectively. For the 20 and 30 bar cases, due to unavailability of the measured integral length scale, a constant $l_x = 1.17$ mm is assumed. With pressure rise from 1 to 10 bar, experiments showed a significant increase in s_T/s_L, espe-

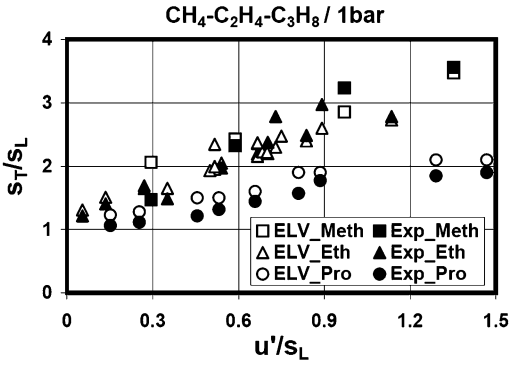

Fig. 4. Flame angles in s_T/s_L from the tLV model for CH_4 ($\phi = 0.9$), C_2H_4 ($\phi = 0.7$), and C_3H_8 ($\phi = 0.9$) flames at 1 bar.

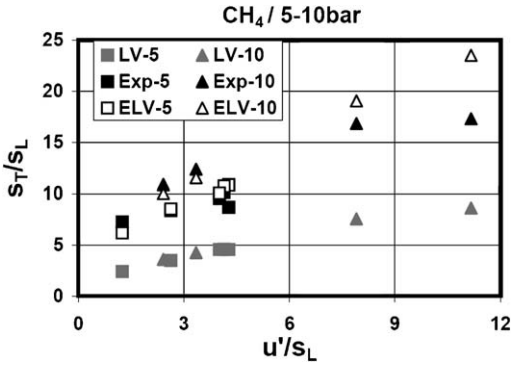

Fig. 5. Measured and calculated flame angle in s_T/s_L (LV and tLV) for methane flames ($\phi = 0.9$) at 5 and 10 bar.

cially up to 5 bar, whereas the behavior of the LV reaction model remains passive, yielding a single low fit curve (see Fig. 5; note that calculations from the modified model (tLV), which appears in the next section, are already included in the following figures). Clearly, pressure effects are missing in the LV reaction model. For methane flames at still higher pressures, 20 and 30 bar, again a clear difference between experiment and simulation is found (Fig. 6). The ethylene flames, shown in Fig. 7, cover a broad spectrum of experimental data based on a blend of three equivalence ratios (0.5, 0.7, and 0.9) for two different pressures, 5 and 10 bar, with u'/s_L ranging up to 24.0 and turbulent Reynolds numbers as high as $Re_t = 1200$. The versatility of the LV model in yielding responsive qualitative fits over this studied range is shown. However, as was found in the aforementioned section, the LV closure conceals the embedded pressure effects, including the variation in fuel type (Fig. 7). The simulated data on a set of more than 60 flames exhibits too low reaction rates collapsing to a single curve. For propane flames at 5 bar, the model shows quantitative differences, although giving a fairly good

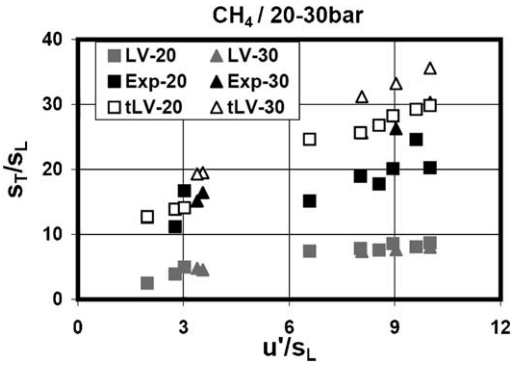

Fig. 6. Methane flame angles ($\phi = 0.9$) at 20 and 30 bar from the LV and tLV reaction models.

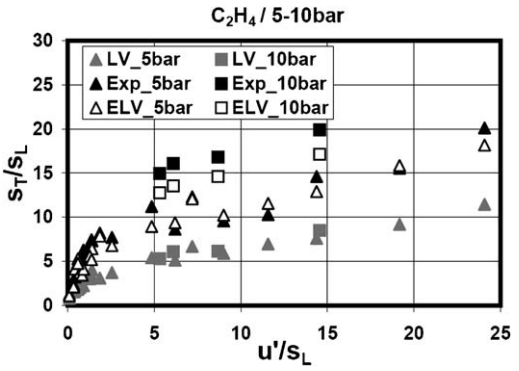

Fig. 7. Ethylene flame angles for three equivalence ratios, $\phi = 0.5$, 0.7, and 0.9 (not distinguished separately), for pressures 5 and 10 bar from the LV and tLV reaction models.

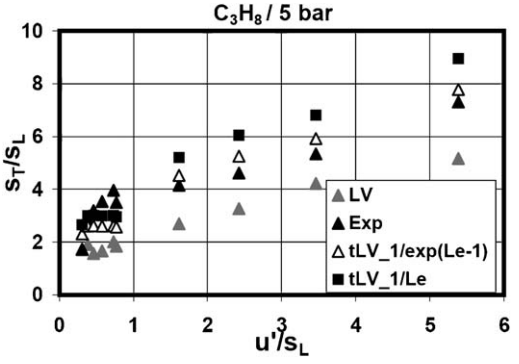

Fig. 8. Propane flame angles ($\phi = 0.9$) at 5 bar using the LV and tLV (calculated using the exponential Lewis number relation, Eq. (11)) models. The square symbols show the turbulent flame speed evaluated using the 1/Le, relation which over predicts at increased turbulence level.

trend, shown in Fig. 8. So far, this comparative study shows that the LV closure gives qualitatively acceptable trends for varied turbulence conditions, witnessing unfavorable quantitative yields, not accommodating the effects of fuel–air mixture and pressure. In the following, this closure is further addressed in its modified form.

4. The tuned Lindstedt–Váos (tLV) reaction closure

Principal objective of this part of the work refers to the LV model in its substantiated form—which we call the tuned Lindtstedt–Váos model (tLV)—by infusing the fuel–air mixture effect and the high-pressure influence. Recall that in the previous section, the LV model in its original form has been shown to underrate the experimental findings, and insists on tuning of the preconstant accordingly. In an earlier study [9], a new preconstant $C_R = 4.0$ for the four measured atmospheric methane–air flame data (Fig. 3) was found, resulting in close proximity to the experimental data. This new value remains as the principal constant for the rest of the investigated data. Interestingly, Gouldin et al. [40] have also proposed $C_R = 4.0$ in their numerical investigation of an oblique flame. Indeed, Lindstedt and Váos assigned a range of values $C_R = 3.25$ to 4.5, if the eddy viscosity turbulent diffusion closure is used [46,51], supporting our choice of the model constant.

4.1. Substantiating the LV model by inclusion of the Lewis number

In practice, fuels of higher molecular weights (usually of high Lewis numbers) than methane have application in spark ignition engines and partly in gas-turbine combustors, so that study of the fuel effects on the flame characteristics at high pressure is of significant importance. A recent experimental and theoretical study on high-pressure flames by Soika et al. [4] affirms the causative important Lewis number effect, highlighting that both flame-generated vorticity and flame instability behavior depend strongly on thermophysical properties of the premixed flame, i.e., effects caused by the density jump and differential diffusive fluxes. It further finds that the Lewis number of the fuel–air mixture has a substantial impact on the extent of flame curvature in the given turbulent flow field. In addition, nonunity Le influence is one of the key parameters in proper understanding of the flame–turbulence interaction [18]. In a recent study by Muppala et al. [16], an explicit Lewis number effect was found for an algebraic reaction rate closure, developed on the concept of turbulent flame–wrinkling ratio. Computed results on the nonunity Le ethylene– and propane–air mixture data using this reaction rate parameter show that there exists an additional difference between experiment and simulation. To reach cooperative agreement for the atmospheric

flame data, the influence of fuel type has been interpreted as a Le effect. Testing several $C_R(\mathrm{Le})$ functions (not produced here) it is found that an exponential Le term,

$$C_{R,\mathrm{Le}} = \frac{4.0}{e^{\mathrm{Le}-1}}, \tag{11}$$

results in very good agreement with the measurements. Fig. 4 shows this impressively for the 40 different atmospheric flames for all the three fuels.

In a previous work, an approximated $C_R \propto 1/\mathrm{Le}$ dependency was used [9]. The difference is small for the methane– and ethylene–air flames, but it is significant for the propane–air flames with $\mathrm{Le} = 1.62$, as can be seen in Fig. 8. The $1/\mathrm{Le}$ relation overpredicts, especially at increased pressure or turbulence level. The empirically found exponential dependency is consistent within the leading point model concepts discussed in a recent review by Lipatnikov and Chomiak [17, pp. 38–48]. They outline the following: (1) Premixed turbulent flame propagation is considered to be controlled by the flamelets that advance farthest into the unburned mixture (the so-called leading points). (2) These leading flamelets are assumed to have an inner structure same as a critically perturbed laminar flame independently on turbulence characteristics. (3) And, a critically curved laminar flame is invoked to model the inner structure of the leading flamelets. Accordingly, turbulent flame speed is controlled by the characteristics of a critically curved laminar flame, rather than by the characteristics of an unperturbed planar laminar flame. To calculate the former characteristics, Lipatnikov and Chomiak [17] have invoked the well-known theoretical solution that predicts that the burning rate in a stationary flame ball (a critically curved laminar flame) is higher than the burning rate in the unperturbed planar laminar flame by a factor of $\exp(1 - \mathrm{Le})$ [52, pp. 327–331; 53]. To elucidate the direct presence and significant impact of the Lewis number, it is of interest to compare typical cases of methane and propane flames with nearly identical flow and turbulence conditions. This is done for a pair of flames (Table 1). Calculated flame cone angles from the LV and tLV models are tabulated in Table 2, showing that the latter model is in good agreement with experiment. For the unity Lewis number flame, the LV model differs by as much as 21.5° with the measured value, with Eq. (11) simplified to $C_R = 4.0$. For the nonunity Lewis number ($\mathrm{Le} = 1.6$) flame this factor results in $C_R = 2.15$, which is marginally close to the original preconstant $C_R = 2.6$. It is worth emphasizing here that fuel–air mixtures characterized by very weak turbulence are not specifically distinguished from the other data here, as s_L remains a strong variant of pressure, but a majority of these flames can be easily classified based on the u'/s_L range.

Table 1
Methane and propane flame data under nearly identical flow and turbulence conditions (pressure in bar, length scale in mm, velocities in m/s)

Fuel	ϕ	p	Le	U	u'	l_x	s_L	u'/s_L
CH_4	0.9	1	1.0	2.36	0.46	1.25	0.34	1.35
C_3H_8	0.9	1	1.62	2.25	0.51	0.9	0.395	1.29

Table 2
Full flame cone angle θ and normalized turbulent flame speed s_T/s_L for the cases described in Table 1

Model/fuel	LV θ°	Exp θ°	tLV θ°	LV s_T/s_L	Exp s_T/s_L	tLV s_T/s_L
CH_4	40	61.5	60	2.37	3.55	3.47
C_3H_8	45.6	38	43	2.21	1.85	2.09

4.2. Intermediate discussion: KPP analysis

In this section, the influence of pressure on reaction rate, interpreted in s_T, is illustrated. These below-discussed relations are not used in the numerical simulations, but only serve to physically interpret the numerical and experimental observations. For this purpose the classical KPP analysis (see [54]) is applied. Here, the balance equation of a one-dimensional steady propagating flame is combined with the LV reaction closure with the assumptions that s_T is equal to the magnitude of the incoming mean velocity, and that turbulence is not affected by the flame:

$$\rho_u s_T \frac{\partial \tilde{c}}{\partial x} = \bar{\rho}\frac{\nu_t}{\sigma_c}\frac{\partial^2 \tilde{c}}{\partial x^2} + C_R \rho_u \frac{s_L}{V_K}\frac{\tilde{\varepsilon}}{\tilde{k}}\tilde{c}(1-\tilde{c}). \tag{12}$$

Assuming that the leading edge of the flame (small $\tilde{c}$) determines the dynamics of the flame (see also [17]), the last term may be expanded ($\tilde{c}(1-\tilde{c}) \to \tilde{c}$), leading to an ordinary differential equation. Following the KPP theorem, this has a physical solution for s_T, if its discriminant is zero [54], leading to

$$s_T = 2\sqrt{\frac{\nu_t}{\sigma_c} C_R \frac{s_L}{\nu_u^{0.25}}\frac{\varepsilon^{0.75}}{k}}. \tag{13}$$

Assuming turbulence parameters (k, ε, and ν_t) to be independent of pressure (a suitable first-order approximation), and with the pressure-dependent quantities $\nu_u \propto p^{-1.0}$ and $s_L \propto p^{-0.5}$ (for methane–air flames), the overall pressure influence on s_T shrinks to

$$s_T \propto p^{-0.125}. \tag{14a}$$

This analysis implies that s_T (or reaction rate) would decrease with pressure, unlike theoretical [17] and experimental findings [2,4–6]. For the two nonunity Le flames (with approximately $s_L \propto p^{-0.25}$),

$$s_T \propto p^{0}. \tag{14b}$$

Following Figs. 5–8 for methane, ethylene, and propane flames, a large gap has been found between experimental and calculated values, with the differences growing larger with pressure rise. Also, computed results based on the corrected factor of $C_R = 4.0$ could not account for the influence of pressure (these intermediate results are not presented here explicitly). Thus, both theory and comparative studies using the simulation and measured data necessitate that an additional (pressure) influence be accommodated into the model.

4.3. Substantiating the LV model for pressure influence

A set of nine methane flames for two high pressures, 5 and 10 bar, are simulated and analyzed independently, with the aim of unveiling the influence of pressure. For 5 bar, with an additional multiplicative correction factor of 2.2 (thus $C_R = 4.0 \times 2.2 = 8.8$), calculated angles are found to be near the measured ones. Similarly, for 10 bar, following a few iterative trials a reasonable but a still bigger factor, $C_R = 4.0 \times 3.1 = 12.4$, is realized. These additional correction factors fit rather well to a supplemental pressure-dependent factor,

$$\bar{w}_c \propto \left(\frac{p}{p_0}\right)^{0.5}, \tag{15a}$$

where p is the operating pressure, with $p_0 = 1$ bar. These calculated flame angles are plotted in Fig. 5 (tLV calculation). As can be seen, experiment and the tLV model are in good agreement with each other, with few exceptions at high turbulence.

In terms of the KPP analysis, a pressure dependency of the turbulent flame speed is thus

$$s_T \propto p^{0.125} \tag{15b}$$

for lean methane–air flames. This value is relatively near to the experimentally found exponent of 0.07 (see Table 3). This explicit pressure influence may be related to a more fundamental quantity, the molecular kinematic viscosity $\nu(\propto 1/p)$, as it is scaled closely to the small scales of turbulence and laminar flame thickness. Therefore a correction factor $\nu^* = \nu/\nu_0 (= p_0/p)$ is interpreted with the modified reaction source term as $\bar{w}_c \propto 1/\sqrt{\nu^*}$, with subscript 0 being the corresponding atmospheric value. With the pressure-dependent term Eq. (15a), calculations are performed for the other 17 high-pressure 20- and 30-bar data. Though the results are not so favorable in retaining the correct quantitative trends (see Fig. 6), they seem promising in a first-order approximation, and certainly give much better results than the actual values. For ethylene and propane flames, the LV model pronounces a pressure-independent reaction rate (see Figs. 7 and 8 and Eq. (14b)), whereas experiments place an $s_T \propto p^{0.24–0.26}$ dependency. Here, the pressure-dependent reaction rate (Eq. (15a)) from the theoretical KPP analysis leads to

$$s_T \propto p^{0.25}. \tag{16}$$

In Table 3 these theoretically derived pressure dependencies for the three fuels are compared with the experimental fits between 1 and 10 bar. The exponents of the tLV model are fairly near to the experimental ones.

Combining this pressure dependency (Eq. (15a)) with the earlier discussed Lewis number effect (of Eq. (11)), the simulated flame data show reasonable agreement to the experimental data for the large set of data points from ethylene and propane flames (Figs. 7 and 8) under varied turbulence conditions. For the ethylene flames, the calculations for 5 bar cases are very near to the measurements, while somewhat underestimating for 10 bar (Fig. 7). For the propane flames at 5 bar (Fig. 8) the tLV model gives rather good results in conjunction with the mentioned exponential Lewis number dependency, leading only to a slight overprediction at higher turbulence intensity. Following these studies, we conclude that this tuned LV model is found to give fairly good quantitative results so far for the broad set of nearly 100 experimental flames. These numerical results are well supported via theoretical argumentation. In summary, the tuned Lindstedt–Váos (tLV) reaction model is given as

$$\bar{w}_c = C_R C_{P,Le}\, \rho_u \frac{s_L^0}{V_K} \frac{\tilde{\varepsilon}}{\tilde{k}} \tilde{c}(1-\tilde{c}), \quad \text{with } C_R = 4.0$$
$$\text{and} \quad C_{P,Le} = \sqrt{\frac{p}{p_0}} \left(\frac{1}{e^{Le-1}}\right), \tag{17}$$

including the explicit influence of both fuel type (via Lewis number) and pressure.

Two supportive verification studies are carried out and are described briefly in the following. The first is to investigate the influence of the turbulent flux model. In the second, the behavior of the reaction closure in spatially uniform turbulence fields is studied.

Table 3
Pressure dependency of turbulent flame speed: LV model, Experiment (Kobayashi), and tLV model

$s_T \propto p^x$, $x =$	LV	Experiment	tLV
CH_4–air (Le = 1.0)	−0.25	0.07	0.125
C_2H_4–air (Le = 1.2)	0.01	0.24	0.26
C_3H_8–air (Le = 1.62)	−0.01	0.25	0.25

Table 4
Inlet flow and flame conditions and experimental and calculated flame angles (s_T/s_L) for varied Schmidt number (tLV model)

Fuel	ϕ	p	U	u'	s_L	l_x	u'/s_L	s_T/s_L Exp	s_T/s_L tLV ($\sigma_c = 0.7$)	s_T/s_L tLV ($\sigma_c = 1.0$)
CH_4	0.9	1	2.36	0.46	0.340	1.25	1.35	3.55	3.47	2.88
	0.9	5	2.21	0.40	0.152	1.15	2.63	8.38	8.52	7.64
	0.9	10	2.11	0.36	0.108	1.10	3.35	12.34	11.54	11.6
C_2H_4	0.5	5	6.95	1.64	0.086	1.40	19.17	15.55	15.85	12.64
	0.7	5	7.53	1.75	0.243	1.50	7.19	12.32	12.08	10.85

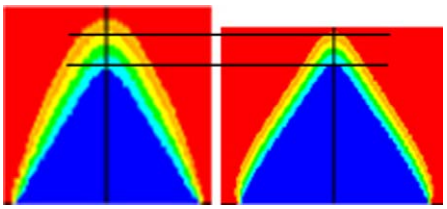

Fig. 9. The weak influence of the Schmidt number σ_c (= 0.7 and 1.0, respectively, for left and right flames) on the turbulent flame speed is shown for a lean methane–air mixture ($\phi = 0.9$, $u'/s_L = 2.63$), using the tLV model.

4.4. Eddy viscosity turbulent diffusion closure

In the original work of Lindstedt and Váos, the turbulent flux term has been treated with second moment balance equations [12], while in the current study it is restricted to the use of gradient closure of $\overline{\rho u'' c''}$ with the standard eddy viscosity approach, with turbulent diffusion coefficient ν_t/σ_c. Váos [46] has investigated the difference between the two approaches, as mentioned in the beginning. Here, we varied σ_c in order to understand the influence of diffusion coefficient on the computed s_T. The value of σ_c is usually taken as either 0.7 or 1.0 (our standard calculations were based on $\sigma_c = 0.7$). For a set of six test flames with different fuels and pressures, the calculated as well as experimental s_T values are given in Table 4 for the two Schmidt numbers σ_c. A decreasing influence of σ_c on s_T with turbulence is observed. Fig. 9 shows a typical calculated methane flame in reaction progress contours for $\sigma_c = 0.7$ and 1.0 at 5 bar from Table 4.

This study reveals that the flame cone angle shows no visible variation with σ_c at moderate turbulence, and that its effect decreases with u'/s_L. But it is likely to influence the flame brush thickness marginally. This analysis supports so far the usage of simplified eddy viscosity closure for turbulent scalar flux.

4.5. Behavior of the reaction closure in spatially uniform turbulence field

An open question that deserves further investigation is the influence of the numerically calculated flame on the modeled turbulence in the variable density case. In order to get some indication of this influence, we compared in a supplemental study few numerical flame angles and corresponding mean velocities with those obtained, for spatially uniform turbulent flow fields. A comparison is shown in Fig. 10 for the three methane flames in Table 4. The mean flame shapes are essentially similar compared to the cases of variable densities. A slight difference in flame brush, broadening along the entire flame region for the high-pressure case, is seen. The computed turbulent flame speed from both the turbulent flow situations remains more or less unchanged. The mean velocity magnitude is affected within the marginally acceptable level. In overall, the cross influence between reaction and turbulence model is not very significant.

4.6. Delimits of the tLV model

Applying the tuned LV model, it is found that simulated flame data differ from measurements at very weak turbulence level at elevated pressures. For a few such flames falling in the range $u'/s_L < 1$ at and beyond 5 bar, the calculated flames are partly suppressed to a flat flame at the very exit of the nozzle (similar to "numerical flashback" due to overpredicted reaction rate). On the other hand, the propane flames at 5 bar have been found with underpredicted flame angles. It should be noted that for very low turbulence intensities the rather complex phenomenon of laminar flame instabilities, as well as possible mismodeling of eventually relaminarized turbulence may be of additional importance. Lindstedt and Váos [12] proposed an empirical procedure, formally adopted from Sreenivasan [55], for low-turbulent flows. This method evaluates the reaction rate via an exclusive expression for the outer cut-off (integral length) scale, $l_x = C_L u'^3/\varepsilon$, where $C_L(\mathrm{Re}_\lambda)$, in order to reconcile calculations and experiments. Allowance of this approach to the current data has not benefited, so far (not shown here) that the results were found inconsistent over the span of very weak turbulence data.

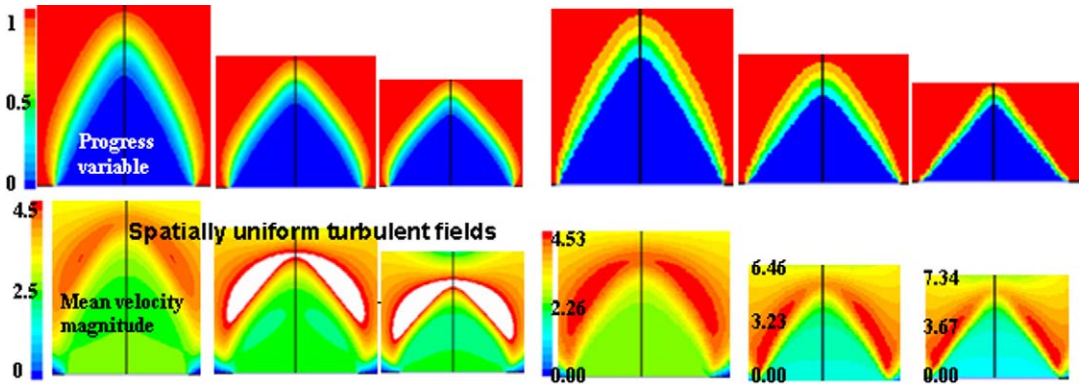

Fig. 10. Influence of the numerical effect on flame-generated turbulence. Three cases: methane–air at 1, 5, and 10 bar (from left to right). Top row: reaction progress variable. Bottom row: mean velocity magnitude. Left block: spatially uniform turbulence field. Right block: variable-density nonuniform turbulence field. White regions in the velocity magnitude in the second and third contours from left correspond to velocities higher than the shown maximum scale of 4.5 m/s.

It is therefore necessary that special care be taken in simulating flames at very low turbulence, which seems to be the case with any other existing reaction model when used in conjunction with the standard k–ε turbulence model. Whether or not the proposed fuel influence is sufficient also for other fuels (or for stoichiometric or even fuel-rich mixtures) has remained beyond the scope of the current work.

5. Conclusions

A formally simple algebraic reaction rate closure derived from fractal flame analysis proposed by Lindstedt and Váos (LV model) was extensively studied for a broad set of turbulent premixed Bunsen flames. The comparison was based on data of nearly 100 flames, consisting of lean methane–, ethylene–, and propane–air mixtures for pressures up to 10 bar (partly 30 bar) and for a wide range of turbulence and flow conditions, $u'/s_L \leqslant 24$. For comparison, essentially the mean flame position of the Bunsen flames, described as the mean flame cone angle, or in dimensionless form as s_T/s_L, was used.

With the original fractal reaction closure (LV model), for model constant $C_R = 2.6$, the calculated atmospheric methane–air flames showed underprediction of reaction rates. Here, tuning to $C_R = 4.0$ was found essential. With this new value, however, ethylene and propane flames were overpredicted, with the differences being fuel-dependent. Following comparison with the experimental set of data as well as based on theoretical arguments, these differences were attributed to the nonunity Lewis number (Le > 1) of the fuels. A new term was successfully introduced, modeling the reaction rate as proportional to $\exp(1 - \mathrm{Le})$.

In case of high-pressure flames, the LV model always underpredicted the mean reaction rate, with growing differences with pressure. Through a systematic semiempirical approach based on the set of 5- and 10-bar methane–air flame data, the multiplicative pressure term $\sqrt{p/p_0}$ substantiated the model significantly. This relation yielded acceptable trends even at higher pressures (20 and 30 bar of methane–air flames).

For other fuels (ethylene and propane, besides methane) at varied pressures, the combined prefactor $\exp(1 - \mathrm{Le})\sqrt{p/p_0}$ added to the LV closure has been found to be in very good terms for most of the investigated flames under varied flow and turbulence levels.

This tuned LV reaction model includes now two important phenomena of technical relevance—the Lewis number effects for different fuels and the influence of high pressure on the reaction rate.

Acknowledgments

We are grateful to Hideaki Kobayashi (Tohoku University, Japan) for providing us with his experimental flame data. This work was funded in the frame of the Bavarian Research Cooperation FORTVER, hosted by the Arbeitsgemeinschaft Bayerischer Forschungsverbünde abayfor.

References

[1] K.N.C. Bray, Proc. Combust. Inst. 26 (1996) 1–26.
[2] H. Kobayashi, T. Nakashima, T. Tamura, K. Maruta, T. Niioka, Combust. Flame 108 (1997) 104–117.
[3] A. Bounif, A. Aris, I. Gökalp, Int. J. Therm. Sci. 38 (1999) 819–831.

[4] A. Soika, F. Dinkelacker, A. Leipertz, Combust. Flame 132 (3) (2003) 451–462.
[5] T. Lachaux, F. Halter, C. Chauveau, I. Gökalp, I.G. Shepherd, Proc. Combust. Inst. 30 (2005) 819–826.
[6] P. Griebel, R. Schären, P. Siewert, R. Bombach, A. Inauen, W. Kreutner, ASME Paper No. GT2003-38398, 2003.
[7] S.P.R. Muppala, N.K. Aluri, F. Dinkelacker, in: Proceedings of the European Combustion Meeting, Louvain-la-Neuve, Belgium, 2005, Paper No. 126, pp. 1–6.
[8] N.K. Aluri, S. Qian, S.P.R. Muppala, F. Dinkelacker, in: Proceedings of the European Combustion Meeting, Louvain-la-Neuve, Belgium, 2005, Paper No. 132, pp. 1–6.
[9] N.K. Aluri, P.K.G. Pantangi, S.P.R. Muppala, F. Dinkelacker, Flow Turbulence Combust. 75 (2005) 149–172.
[10] V.L. Zimont, A.N. Lipatnikov, Chem. Phys. Reports 14 (7) (1995) 993–1025.
[11] K.N.C. Bray, Proc. R. Soc. London A 431 (1990) 315–335.
[12] R.P. Lindstedt, E.M. Váos, Combust. Flame 116 (1999) 461–485.
[13] R.S. Cant, S.B. Pope, K.N.C. Bray, Proc. Combust. Inst. 23 (1990) 809–815.
[14] J.M. Duclos, D. Veynante, T. Poinsot, Combust. Flame 95 (1993) 101–117.
[15] T. Mantel, R. Borghi, Combust. Flame 96 (1994) 443–457.
[16] S.P.R. Muppala, N.K. Aluri, F. Dinkelacker, A. Leipertz, Combust. Flame 140 (2005) 257–266.
[17] A.N. Lipatnikov, J. Chomiak, Prog. Energy Combust. Sci. 31 (2005) 1–71.
[18] Y.-C. Chen, R.W. Bilger, Combust. Flame 131 (4) (2002) 400–435.
[19] B. Renou, A. Boukhalfa, D. Puechberty, M. Trinité, Combust. Flame 123 (4) (2000) 507–521.
[20] T. Brutscher, N. Zarzalis, H. Bockhorn, Proc. Combust. Inst. 29 (2002) 1825–1832.
[21] A. Trouvé, T. Poinsot, J. Fluid Mech. 278 (1994) 1–31.
[22] H. Kobayashi, T. Tamura, K. Maruta, T. Niioka, Proc. Combust. Inst. 26 (1996) 389–396.
[23] H. Kobayashi, Y. Kawabata, K. Maruta, Proc. Combust. Inst. 27 (1998) 941–948.
[24] H. Kobayashi, List of Experimental Data of High Pressure Flames, personal communication, 2001.
[25] T. Poinsot, D. Veynante, S. Candel, Proc. Combust. Inst. 23 (1990) 613–619.
[26] C. Meneveau, T. Poinsot, Combust. Flame 86 (1991) 311–332.
[27] F. Dinkelacker, A. Soika, D. Most, D. Hofmann, A. Leipertz, W. Polifke, K. Döbbeling, Proc. Combust. Inst. 27 (1998) 857–865.
[28] F. Dinkelacker, Struktur turbulenter Vormischflammen, Habilitation thesis, Universität Erlangen, Berichte zur Energie- und Verfahrenstechnik (BEV), Heft 1.4, Esytec, Erlangen, 2001.
[29] F. Dinkelacker, in: Proceedings of the European Combustion Meeting, Orleans, France, 2003, Paper No. 158, pp. 1–6.
[30] N. Peters, Turbulent Combustion, Cambridge Univ. Press, Cambridge, UK, 2000.
[31] N. Peters, J. Fluid Mech. 384 (1999) 107–132.
[32] F.A. Williams, Combustion Theory, second ed., Addison–Wesley, Reading, MA, 1985.
[33] N. Peters, Proc. Combust. Inst. 21 (1986) 1231–1250.
[34] F.C. Gouldin, Combust. Flame 68 (1987) 249–266.
[35] K.N.C. Bray, in: P.A. Libby, F.A. Williams (Eds.), Turbulent Reacting Flows, Springer-Verlag, Berlin, 1980, pp. 115–183.
[36] H.G. Weller, S. Uslu, A.D. Gosman, R.R. Maly, R. Herweg, B. Heel, COMODIA 94 (1994) 163–169.
[37] X. Zhao, R.D. Matthews, J.L. Ellzey, COMODIA 94 (1994) 157–162.
[38] A.R. Kerstein, Proc. Combust. Inst. 21 (1988) 1281–1290.
[39] F.C. Gouldin, K.V. Dandekar, AIAA J. 22 (1984) 655.
[40] F.C. Gouldin, K.N.C. Bray, J.-Y. Chen, Combust. Flame 77 (1989) 241–259.
[41] R.P. Lindstedt, V. Sakthitharan, in: 8th Symposium on turbulent shear flows, Technical University of Munich, Germany, 1991.
[42] Ö.L. Gülder, G.J. Smallwood, R. Wong, D.R. Snelling, R. Smith, B.M. Deschamps, J.-C. Sautet, Combust. Flame 120 (4) (2000) 407–416.
[43] Ö.L. Gülder, G.J. Smallwood, Combust. Flame 103 (1995) 107–114.
[44] F. Charlette, C. Meneveau, D. Veynante, Combust. Flame 131 (1–2) (2002) 159–180.
[45] M. Murayama, T. Takemo, Proc. Combust. Inst. 22 (1988) 551–559.
[46] E.M. Váos, Second Moment Methods for Turbulent Flows with Reacting Scalars, Ph.D. thesis, Imperial College, University of London, 1998.
[47] R.G. Abdel-Gayed, D. Bradley, M.N. Hamid, M. Lawes, Proc. Combust. Inst. 20 (1984) 505–512.
[48] Fluent, Fluent Incorporated, Lebanon, NH, USA, 2003.
[49] K.N.C. Bray, P.A. Libby, J.B. Moss, Combust. Flame 61 (1985) 87–102.
[50] S.P.R. Muppala, F. Dinkelacker, Prog. Comput. Fluid Dynamics 4 (6) (2004) 328–336.
[51] R.P. Lindstedt, private communication, 2004.
[52] Y.B. Zel'dovich, G.I. Barenblatt, V.B. Librovich, G.M. Makhviladze, The Mathematical Theory of Combustion and Explosions, Plenum, New York, 1985.
[53] B. Rogg, in: N. Peters, J. Warnatz (Eds.), A GAMM—Workshop 'Numerical Methods in Laminar Flame Propagation,' Vieweg & Sohn, Braunschweig/Wiesbaden, 1981, pp. 38–48.
[54] T. Poinsot, D. Veynante, Theoretical and Numerical Combustion, Edwards, Philadelphia, 2001.
[55] K.R. Sreenivasan, Phys. Fluids A 27 (5) (1984) 1048–1051.